Energy Technology

Generation, Conversion, Storage, Distribution

Accepted Article

Title: An Improved Multi-Evaporator Adsorption Desalination Cycle for GCC Countries

Authors: Muhammad Wakil Shahzad and Kim Choon Ng

An Improved Multi-Evaporator Adsorption Desalination Cycle for GCC Countries

Muhammad Wakil Shahzad and Kim Choon Ng

Water Desalination and Reuse Centre,
King Abdullah University of Science & Technology,
Thuwal, 23955-6900, Saudi Arabia.
Muhammad.shahzad@kaust.edu.sa, kimchoon.ng@kaust.edu.sa

Table of Content:

The cascaded evaporator adsorption desalination cycle is one the most efficient desalination process operated with industrial waste heat or solar energy. The overall recovery can reach up to 80-85% because of low temperature operation. One of the highest recovery and lowest specific energy consumption desalination process reported in the literature up till now.

1
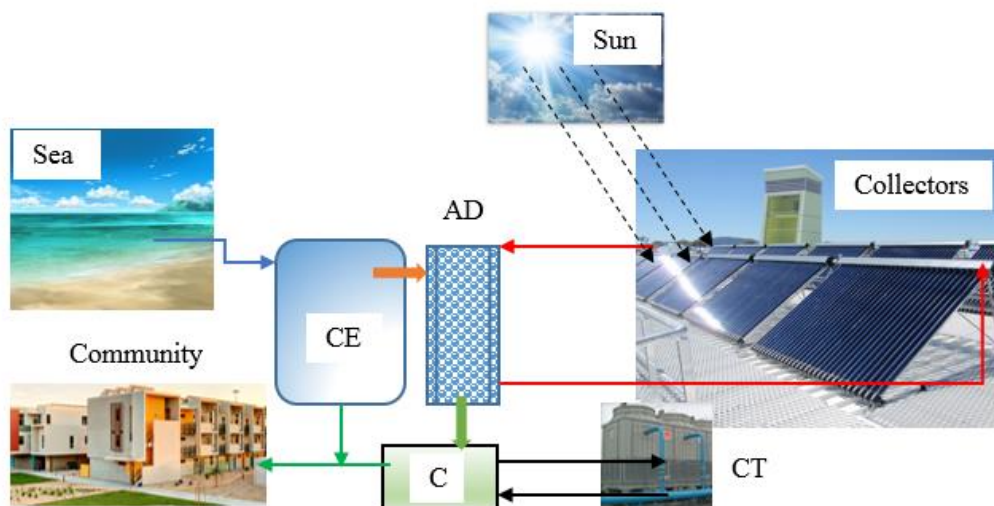
Abstract:

In Gulf Cooperation Council (GCC) countries, cogeneration based desalination processes consume almost 25% of the total annual energy and it is increasing at 2.2% annually. The high fresh water demand is attributed to high gross domestic product (GDP) growth rate, 24%, and the high water languishes, more than 10%. Over the past two decades, GCC countries have spent tens of billion dollars to expand their present and planned desalination capacities. It is foreseeable that with business-as-usual scenario, the domestic oil consumption of Saudi Arabia may exceed its production capacity by 2040. Innovative and sustainable water production solutions are needed urgently for future water supplies without environment impact. In this paper, a hybrid desalination cycle is proposed by integrating multi cascaded-evaporators (CE) with an adsorption cycle (AD). In this new innovative cycle, AD desorbed vapors are supplied to the CE to exploit the latent condensation energy within the evaporators arranged in both pressures-temperatures cascaded manner to improves the performance ratio (PR) of the cycle. Hybrid cycle shows more than 10 folds water production improvement as compared to conventional AD cycle due to synergetic effect. This concept is demonstrated in a laboratory pilot plant using a 3 cascaded evaporators pilot and simulation of 8 evaporators hybrid cycle.

Keywords: Energy efficiency, Sustainable desalination, Thermal desalination, Adsorption cycle.

2

1-   Introduction

The current economic growth is expected to upsurge global water demand more than 55% by 2050 and major sectors such as manufacturing, power generation and domestic will contribute their shares as 400%, 140% and 130% respectively. This trend will affect 40% of global population by pushing them below water scarcity level, less than 1000m^3 per capita per year.[1-4] The energy intensive desalination processes are the only choice for future global water supplies. Currently, 38 billion m^3 per year water is supplied to 150 countries by more than 18,000 desalination plants. The desalination trend is expected to increase more than 40% by 2030 as compared to 2016.[5-7] Presently, global desalination processes consume 75.2 TWh per year electricity, 0.4% of global production.[8]
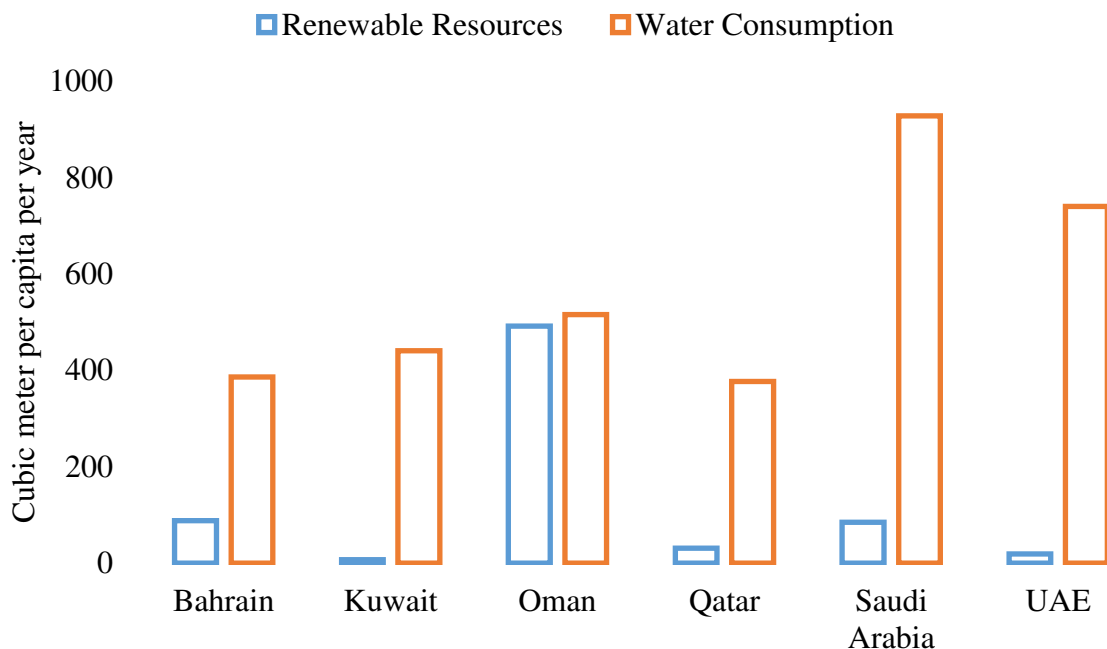

Figure 1: Renewable fresh water availability and water consumption trend in GCC countries. [13]

3

GCC countries are the major shareholders, 39%, of World desalination capacities due arid climate and almost no rain. In GCC countries, Saudi Arabia (SA) is leading with 17% installations producing 13 million cubic meter per day (Mm^3/day) from over 130 desalination plants followed by UAE's 10Mm^3/day production from 100 plants. The water demand in the SA is growing at a rate of 7.5 percent annually pushing the availability of fresh water below 100 m^3 per capita which is far lower than the United nation's water scarcity level.[9-12] The average water availability in GCC countries is shown in Figure 1. [13] Presently, more than 10 private companies including ARAMCO, Marafiq and ACWA Power are producing 42% of desalinated water for SA and the remaining gap is filled by the Saline Water Conversion Corporation (SWCC), the main water authority for supplying potable water of SA, by operating 27 desalination plants. The SA consumes approximately 1.5 million barrels of oil a day for desalination processes and with business-as-usual scenario, the predicted domestic oil consumption of SA may exceed its oil production capacity by 2040. [14]

Thermally driven (MSF & MED) and membrane separation (RO) processes are commercially available desalination technologies covering almost 90% of World market. Their share in desalination sector varies in different part of the World and it depends on feed water quality. Overall, RO processes are leading with 53% share followed by thermally driven technologies 33% and remaining is covered by other emerging processes such as ED, MD and AD etc. In GCC, thermally driven processes contribution is the highest, 56% followed by RO 42%.[15, 16] For energy efficiency and sustainability, the energy planners opted to have desalination plants co-located with power plants to share the same seawater intake and discharge facilities. The independent water and power production (IWPP) installation in Jubail, KSA is the world's largest co-generation facility that produces 2,745 megawatt (MW) power and 800,000 m^3/day desalinated water. [17, 18] The fossil fuel consumption for increasing water and power demand is obviously untenable as it not only affects countries economy in terms of balance of payment but also environment in terms of CO_2 emission. Saudi Arabia ranked 9th globally with 601.9 million tonnes of CO_2 emission in 2014 which was 7.7% higher than 2013 emission level. In per capita emissions, Qatar leading with 60.9 tonnes per year followed by Kuwait and UAE with 26.8 tonnes and 25.2

4

tonnes of CO_2 per capita respectively. In comparison to the world's average 4.9 tonnes of CO_2 emission per capita, Qatar's is 829% above the global average followed by Kuwait 449%, UAE 342% and Saudi Arabia 295%.[19-22] Figure 2 shows the basic economic parameters index trend from 2000 to 2015 in GCC countries. [22]
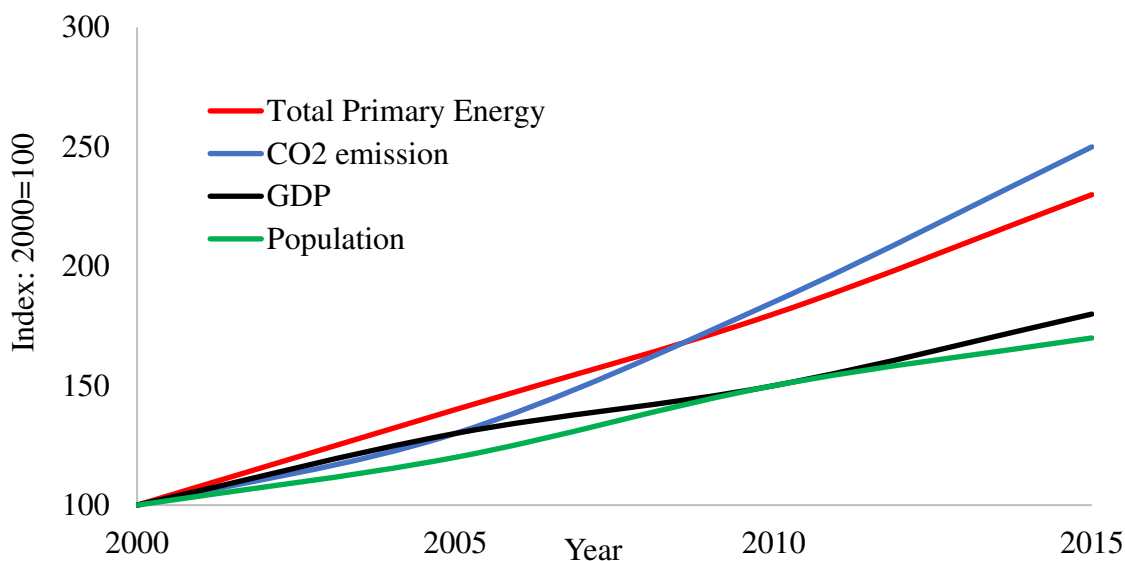

Figure 2: GCC countries important economic parameters index trend from 2000 to 2015. [22]

Considering high energy consumption and CO_2 emission related to desalination in GCC, an innovative desalination methods are required immediately to fulfill future sustainability goal. We proposed an innovative thermal hybrid desalination system that is not only energy efficient but can also handle brine at high concentrations. The cycle comprises a hybridization of Adsorption (AD) cycle and the Cascaded Evaporators (CE) system. Low-grade heat source at 55 °C to 85°C is used to regenerate the adsorbent of an AD cycle and the CE system is operated with desorbed vapor emanating from an AD condenser/desorption bed. This innovative cycle simply called the CE+AD cycle where its advantages include: (i) eliminate additional heat source required for CE system, (ii) reduce cooling tower size, (iii) handle high concentration brine due to low operational temperature, (iv) low evaporative temperature reduce corrosion and fouling chances, (v) low primary energy consumption and minimal carbon foot print

5

because electricity only used to operate liquid, (vi) low grade waste heat or solar renewables can be supplied to AD cycle for adsorbent regeneration and (vii) improve

water production and performance ratio. The detail of hybrid cycle is discussed in following sections.

2- Cascaded Evaporator Adsorption (CE+AD) Cycle

CE+AD is a hybrid of cascaded multi evaporators and adsorption cycle. AD cycle was developed by Ng et al. [23] and it can operate as low as 10°C evaporator temperature using renewable energy or industrial waste heat from 60°C to 80°C for adsorbent regeneration.

2.1-AD Cycle Operational Strategy:

The conventional adsorption cycle is consist of four major components namely; (i) evaporator, (ii) adsorbent beds, (iii)

condenser and (iv) circulation pumps. Feed is supplied to AD evaporator and chilled water is circulated through tubes to maintain saturation temperature. The vapor produced in the evaporator are channeled to the silica gel bed to adsorb on surface of adsorbent. The commercial grade silica gel ($SiO_2.nH_2O$) has a pore surface area of 700–800 m^2/g, and it is available in abundance. SEM picture of mesoporous silica gel and its isotherms are shown in Figure 3 (a & b).
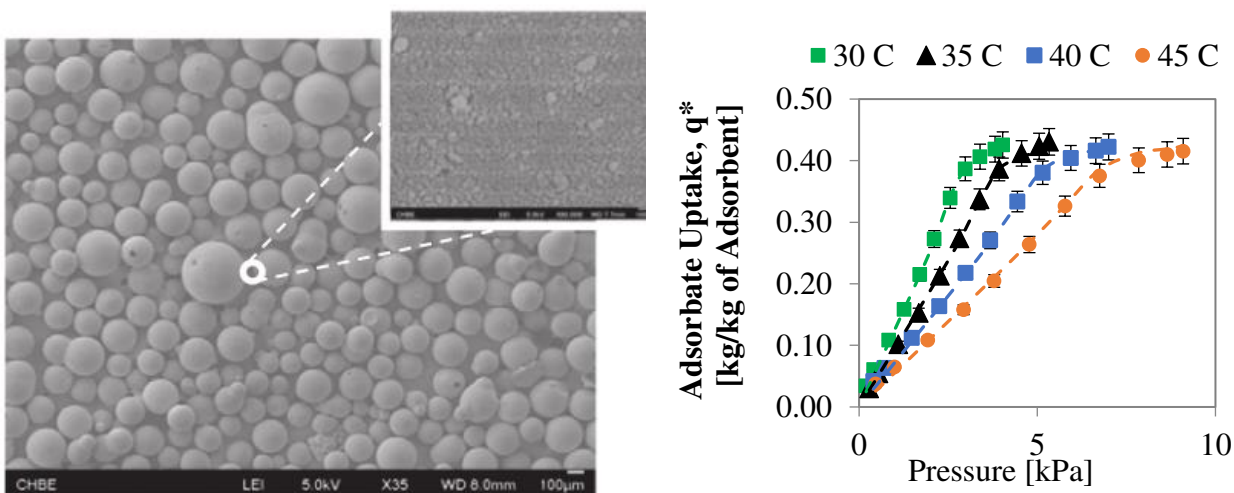

Figure 3: (a) SEM picture of mesoporous silica gel. The insert has a magnification of 80,000 and (b) the isotherms of silica gel at 30 °C to 45 °C at low water vapor (single component) pressures. [28]
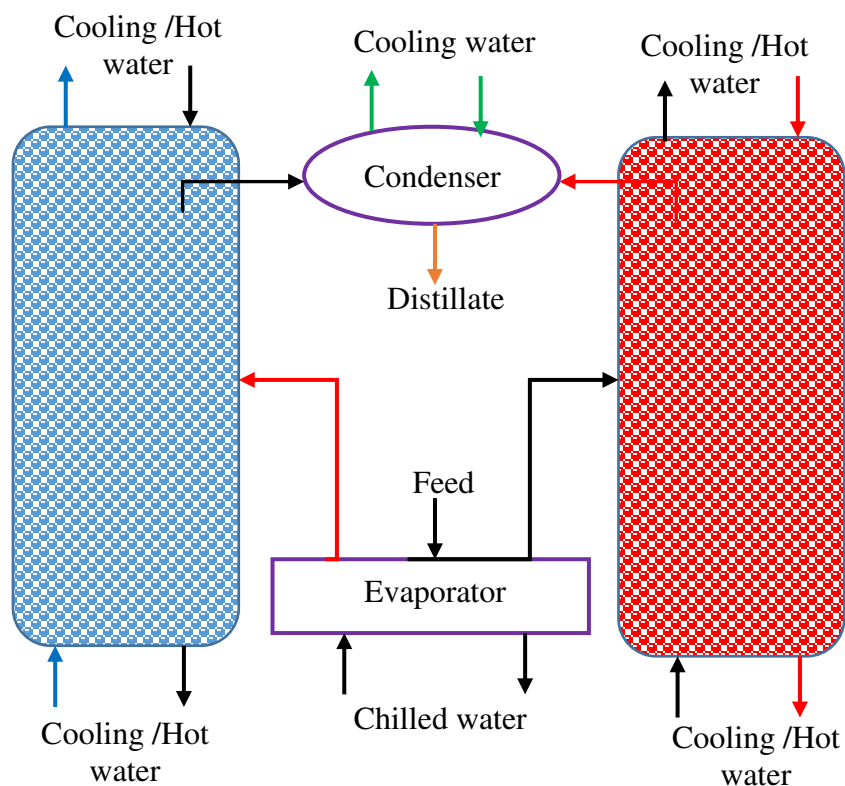
Figure 4: Operational schematic of conventional Adsorption cycle.

Near situation condition, the second bed takeover duties and adsorb vapor produced in the evaporator. At the same time, the hot water is circulated through the tubes of saturated bed to regenerate silica gel to prepare it for next adsorption process. The desorbed vapor are condensed in the condenser and heat is rejected to cooling tower. The process flow schematic is shown in Figure 4. The detail of AD cycle can also be found in the published literature.[24-28] AD cycle can be integrated with other thermally driven desalination system such as MED to improve overall performance. Shahzad et al.[29] conducted theoretical study and simulation of AD cycle integration with MED to extend bottom brine temperature to as low as 10°C as compared to conventional MED condenser at 40°C. Their results showed that MED-AD hybrid can boost water production to almost two fold at same top brine temperature. Shahzad et al. [30-32] also conducted experimental study on MED-AD hybrid at heat source temperature from15°C to 70°C and found good agreement with their theoretical simulation, two fold

7

performance improvement. They concluded that excellent thermodynamic synergy of

integration can allow MED last stages to operate below ambient condition.

2.2-CE+AD Cycle Operational Strategy

It can be observed that in MED-AD integration, MED need separate heat source to maintain top brine temperature (TBT), while in proposed cycle it is recovered from AD process. In proposed new cycle, the heat of condensation from desorbed vapors, emanating from the AD desorption bed, is circulated through the tube side of first evaporator of cascaded-evaporators system. Seawater feed is sprayed onto the tube surface parallel to all evaporators and vapor produced are than channelized to the tube side of next evaporator. This continuous process of vapor production and condensation in successive evaporators continue until the last evaporator that is connected to AD beds to adsorb produce vapor onto the silica gel surface. Distillate from each evaporator is collected in a common header that is connected to

collection tank via u-tube to maintain pressure difference. Similarly, brine is also collected into brine tank from each evaporator. Since system can handle high concentration due to low operational temperature, some of brine is mixed with feed and re-circulated to system to increase recovery ratio as high as 70-80%. Detailed process flow schematic of new cycle is shown in Figure 5. It can be noticed that only low grade waste heat or solar renewable energy from 55°C to 85°C is required to operate AD cycle and cascaded evaporator system input is recovered from AD cycle desorbed vapor condensation. On top of that, condensation heat is re-utilized multi time in cascaded evaporators to boost overall performance. The re-utilization of recovered energy in CE system shows superiority of CE+AD cycle over previously suggested integrations.
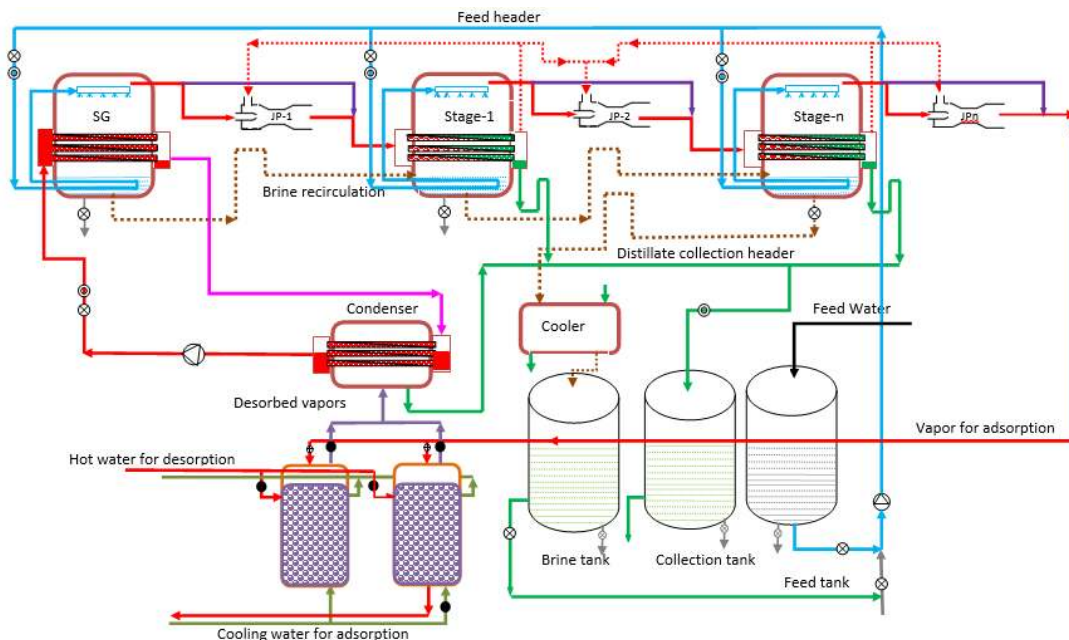
Figure 5: Cascaded evaporators and adsorption cycle hybrid (CE+AD) flow schematic

3- CE+AD Cycle Simulation

Detailed simulation code was built in FORTRAN and International Mathematics and Statistics Library (IMSL) was used to solve differential equations simultaneously using initial value problem solving technique. Detailed mathematical model of hybrid cycle is presented in Appendix A. Heat source temperature and evaporator heat transfer area was used according to estimated experimental pilot, 47C and 4m^2 respectively. For low temperature evaporation modeling, author developed their own falling film heat transfer correlation because of lack of published

data.[33,34] It is found that total 8 number of evaporators can be installed within given operational temperature limit.

Figure 6 shows the temperature profiles of eight evaporators integrated with AD cycle. The heat source temperature and power input was maintained at 47°C and 45 kW. It can be observed that last evaporator temperature was dropped to as low as 4°C due to adsorption effect. The inter-evaporator temperature differential was noted as 3°C to 4°C, showing good agreement with expected experimental results. This temperature differential can be controlled by adsorbent quantity and evaporator design according to

9

number of evaporators. In last few evaporators, cyclic temperature profiles are

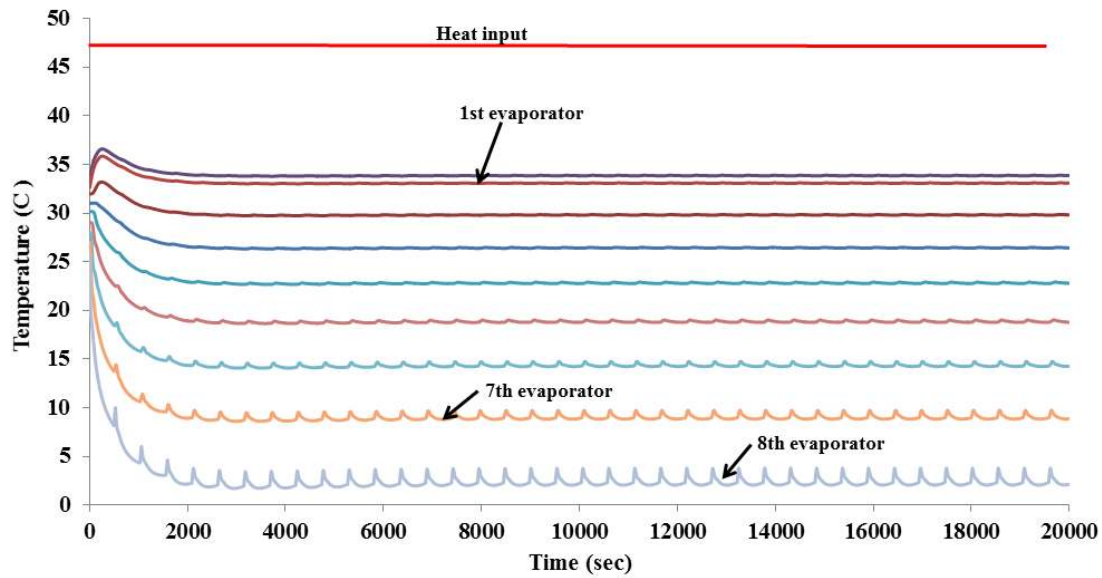due to AD cycle operation that verify experimental temperature profiles

.

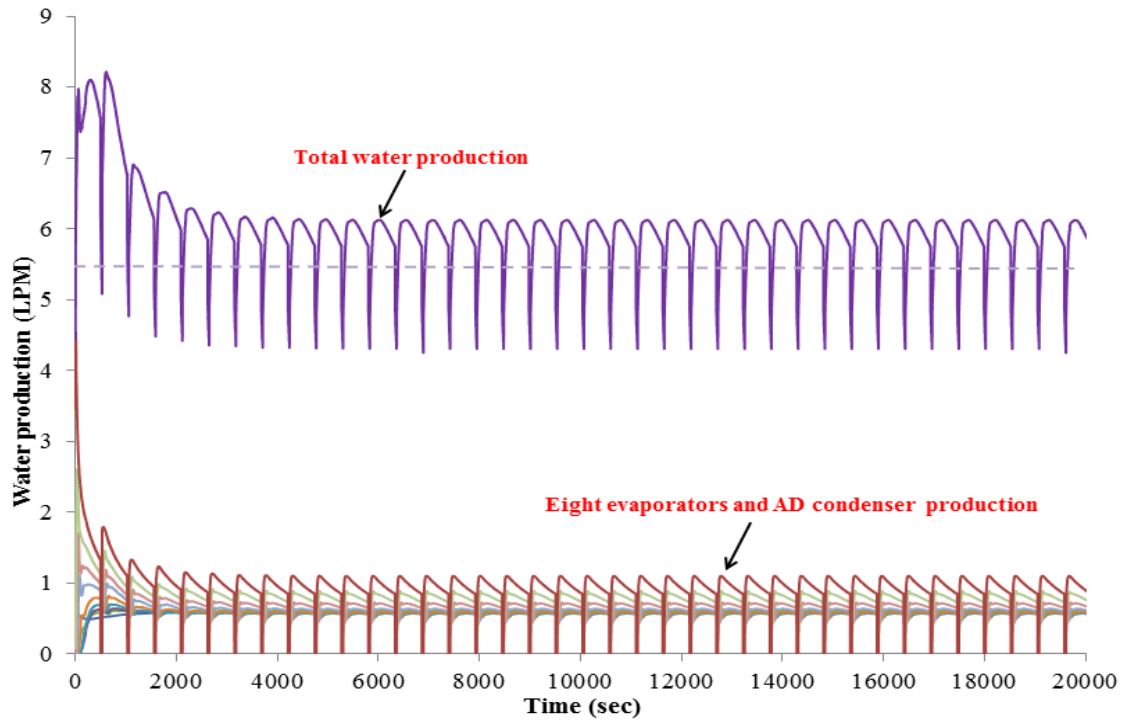Figure 6: Simulation temperature profiles of CE+AD cycle components from start to steady state condition.

Figure 7: Simulation water production profiles of CE+AD cycle and total water production.

10

Figure 7 shows the water production of eight evaporators and AD condenser. Total production is also calculated and average estimated as 5.50LPM as shown by dotted line. Cyclic water production profiles are due to cyclic heat source temperature to each evaporators. It can be observed that thermal energy for CE system is extracted from AD and it is non-payable**.**

4- CE+AD Cycle Experimentation: Results & Discussion

For simulation results verification, a 3 evaporator system integrated with AD cycle was designed, fabricated and installed. Thermal energy required for cascaded-evaporators is recovered from the AD beds desorbed vapor condensation. Temperature profiles of heat source from AD condenser and all evaporators are shown in Figure 8. Steady state temperatures of condenser's cooling water inlet and outlet were observed as 43ºC and 47ºC respectively. The outlet water from condenser, at 47ºC, is supplied to the tube side of first evaporator and return at 43º is supplied back to the condenser. The inter-evaporator temperatures were noted as 3ºC to 4ºC, same as simulation results. The third or last evaporator temperature was observed as 35ºC and it is limited by number of evaporators. It can be as low as 5ºC if more number of evaporators will be installed. The cyclic temperature profiles are due to AD cyclic operation and that is damping down toward last evaporator. Evaporator pressure profiles are shown in Figure 9. It can be seen that all evaporator pressure trends are same as temperature profiles due to saturation conditions.
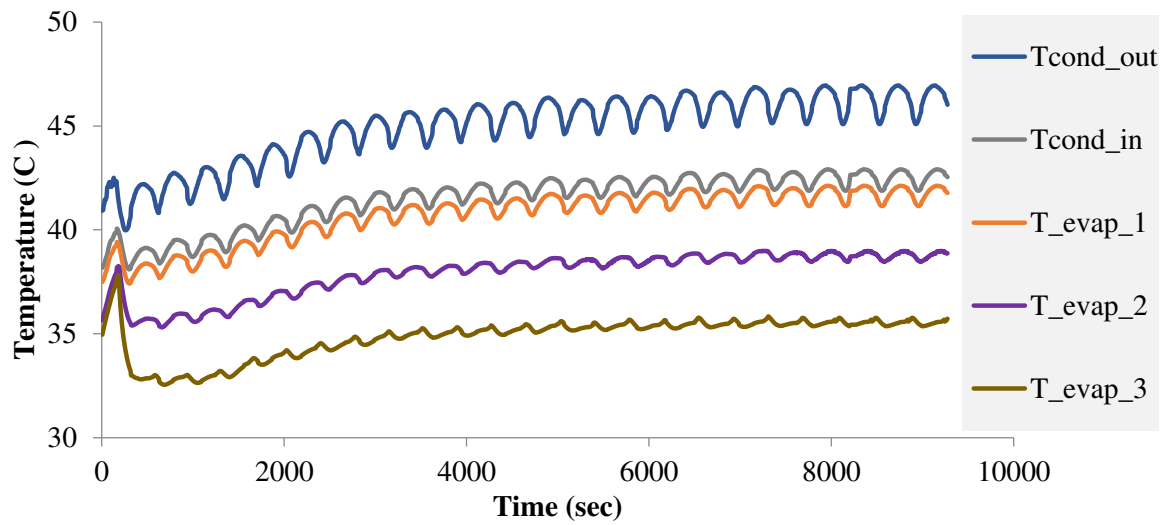
11

Figure 8: Temperature profiles of CE+AD cycle components from start to steady state condition.
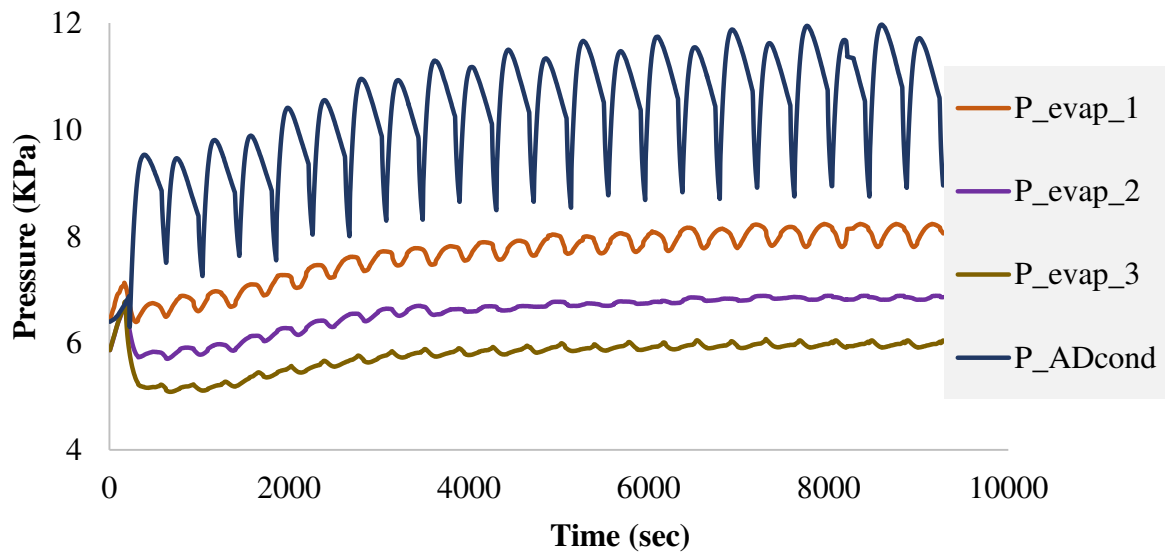

Figure 9: Pressure profiles of CE+AD cycle components from start to steady state condition.

12
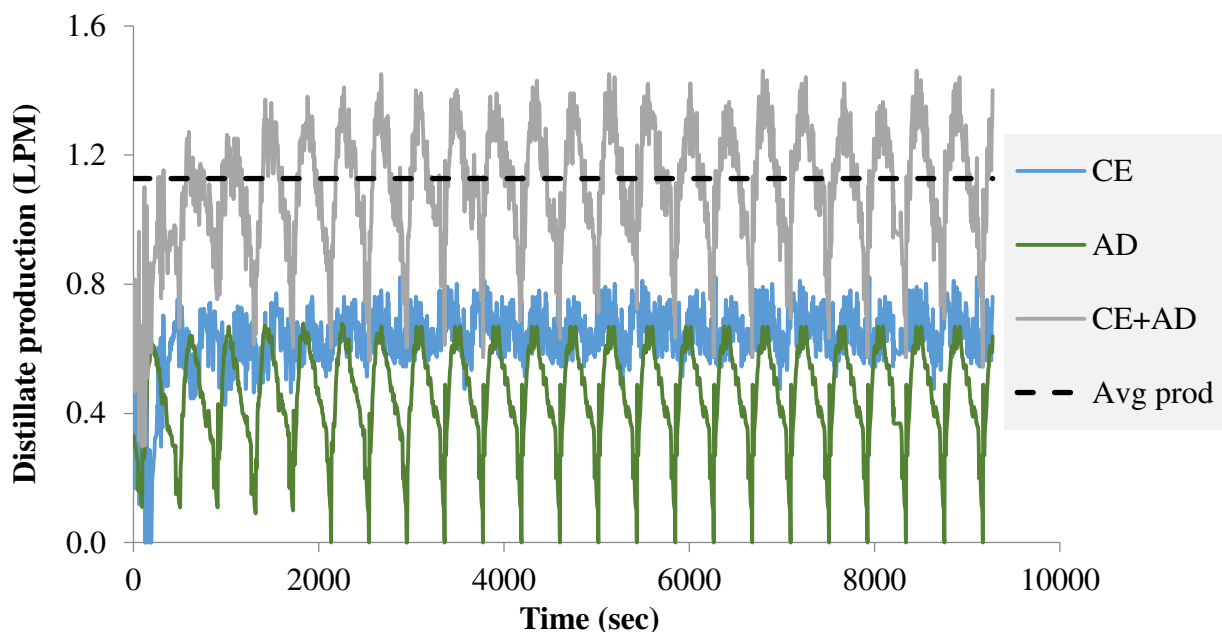
Figure 10: Water production profiles of CE+AD cycle and total water production.

Figure 10 shows the water production profile of CE+AD cycle. The total water production from three cascaded-evaporators operating from desorption recovered heat is noted as 1.15LPM. The cyclic production profile is observed because it follows the temperature profile of heat source. The additional water production from three evaporators is only at expense of electricity consumption for liquid circulation pumps while thermal energy required is recovered from AD vapor condensation. The whole system is stationary except liquid circulation pumps so

this new cycle is not only low operational cost but also very minimal maintenance cost is required.

Figure 11 shows the summary of results. More than two fold water production improvement has been observed with three cascaded evaporator's integration to recover AD vapor condensation energy.

Performance ratio (PR) of basic AD and hybrid CE+AD cycles are also presented. It can be noted that PR improvement is also two folds as compared to basic AD cycle

13
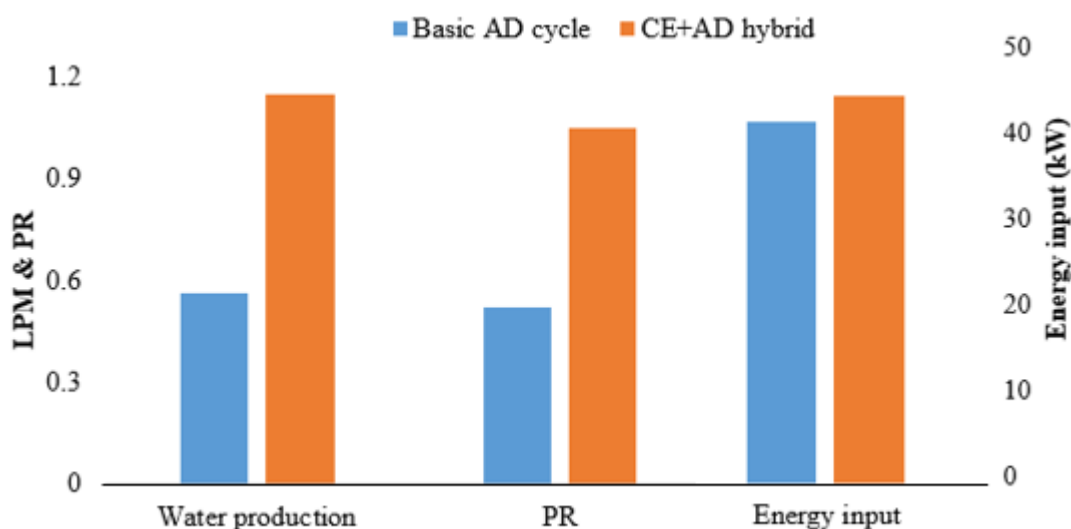
Figure 11: Experimental results comparison of water production, PR and energy input of basic AD cycle and CE+AD cycle.

The comparison between simulated 8 evaporator hybrid cycle, the experiments of the basic AD cycle and three evaporator CE+AD cycle is presented in Figure 12. It can be seen that hybrid cycle improved performance ratio (PR) to almost 10 times as compared to basic AD cycle. This shows that hybridization of cascading evaporators with AD cycle to recover condensation heat can produce additional 10 times water while AD desorption heat is supplied from industrial waste heat or from solar renewables. The conventional evaporators and AD cycle are robust in operation with different feed condition and widely accepted in processes industries. CE+AD cycle concept can be scaled to any size because both technologies are well proven in the industry for different purposes. The proposed cycle operating with waste heat, the electricity only utilized for liquid circulation pumps. It can be the lowest energy and carbon emission (8-10 times) water production cycle as compared to conventional desalination cycle.
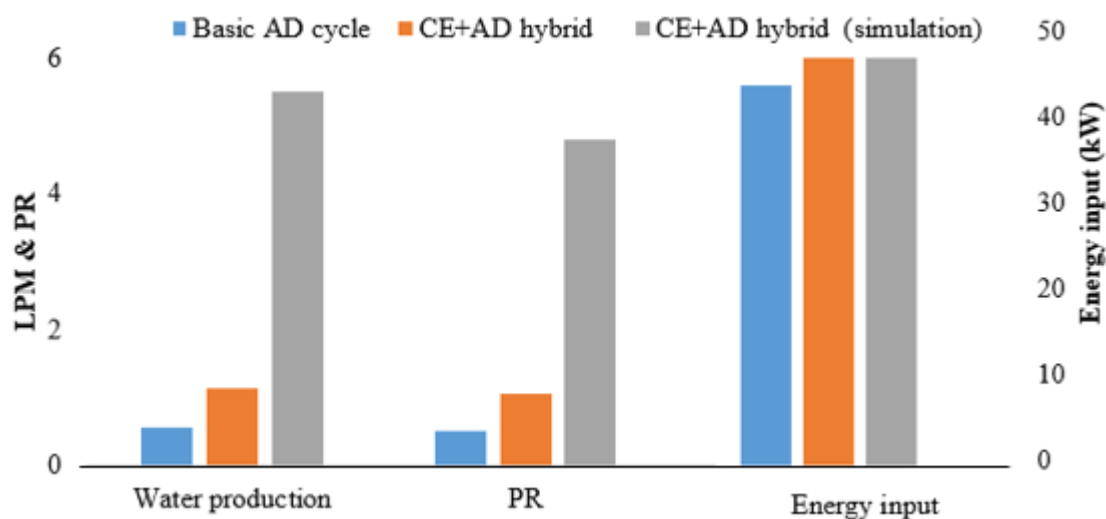
14

Figure 12: Comparison of water production, PR and energy input of basic AD cycle, three evaporator CE+AD cycle experiments and eight evaporator hybrid cycle simulation.

These results, conventional AD cycle and proposed CE+AD hybrid cycle, can be used as a reference for industrial scale design. According to specific requirement, AD cycle can be designed with different number of evaporators. Since cycle is operating with industrial waste heat or renewable energy, it is sustainable solution for future water supplies.

Conclusions

Cascaded evaporator (CE) integration with AD cycle has been proposed to recover heat of condensation and to re-utilize in CE for excellent thermodynamic synergy. An experimental study on three evaporators hybridized with AD cycle was conducted successfully to demonstrate workability of proposed cycle. It shows almost two fold performance improvement as compared to conventional AD cycle. A full scale simulation was also performed to demonstrate industrial scalability. This new proposed hybrid cycle have the performance ratio of about 4.8-5.0 which almost 10 folds of the conventional AD cycle. The hybrid CE+AD cycle is an efficient desalination method with minimal carbon emission.

15

Abbreviations

GDP	Gross domestic product	IWPP	Independent water and power production
GCC	Gulf cooperation countries		
CE	Cascaded-evaporators	SA	Saudi Arabia
PR	Performance ratio	KSA	Kingdom of Saudi Arabia
AD	Adsorption cycle	MW	Megawatt
SWCC	Saline Water Conversion Corporation	LPM	Liter per minute
		IMSL	International Mathematics & Statistics Library

References

1. Water and energy, The United Nations world water development report, **2014**. http://unesdoc.unesco.org/images/0022/002257/225741E.pdf (Accessed 20-01-2017)

2. Water for a sustainable World, The United Nations world water development report, **2015.** http://unesdoc.unesco.org/images/0023/002318/231823E.pdf (Accessed 22-01-2017)

3. UN Stresses Water and Energy Issues, World Water Day 2014 Report, 2014. https://unu.edu/media-relations/releases/wwd2014-un-stresses-water-energy-issues.html (Accessed 22-01-2017)

4. Water and Energy: Facts and Figures, The United Nations World Water Development (WWDR) Report, **2014**. http://www.unesco.org/fileadmin/MULTIMEDIA/HQ/SC/pdf/WWAP_WWDR4%20Facts%20and%20Figures.pdf (Accessed 25-01-2017)

5. Desalination by the Numbers, International desalination association, **2016**. http://idadesal.org/desalination-101/desalination-by-the-numbers/ (Accessed 26-01-2017).

6. N. Ghaffour, T. M. Missimer, G. L. Amy, Desalination **2013**, 309,197–207.

7. M. Elimelech, W. A. Phillip, Science, **2011**,333, 712-717.

8. UN Water Report, The United Nations inter-agency mechanism on all related issues, including sanitation, **2014**. http://www.unwater.org/statistics/statistics-detail/es/c/211827/. (Accessed 20-01-2017)

9. M. W. Shahzad, K. C. Ng, Nature Middle East, **2016**, doi: 10.1038/nmiddleeast.2016.50.

10. M. A. Dawoud, Desalination **2005**, 186, 187-198.

11. A. Siddiqi, L. D. Anadon, Energy Policy **2011**, 39, 4529-4540.

12. M. A. Dawoud, Environment and Sustainability, **2012**, 1, 27-35.

13. Achieving a sustainable water sector in the GCC: Managing supply and demand, building institutions, A report by Strategy&, **2014**. http://www.strategyand.pwc.com/reports/achieving-sustainable-water-sector-gcc (Accessed 20-01-2017)

14. H. Fatha, A. Sadikb, T. Mezhera, Thermal & Environmental Engineering, **2013**, 5, 155-165.

15. A. Nasser Mabrouk, H. E.S. Fath, Desalination, **2015**, 371, 115–125.

16

16. T. Mezher, H. Fath, Z. Abbas, A. Khaled, Desalination, **2011**, 266, 263–273.

17. World largest desalination plant in Saudi arabia, **2009**.
https://www.greenprophet.com/2009/05/saudi-arabia-desalination/
(Accedded 27-01-2017)

18. Marafiq IWPP, Saudi Arabia, **2014**.
http://www.sidem-desalination.com/main-references/main-references/Marafiq/
(Accedded 27-01-2017)

19. M. W. Shahzad, M. Burhan, L. Ang and K. C. Ng, Desalination, **2017**, 413, 52-64.

20. M. R. Qader, Energies, **2009**, 2 1201-1213.

21. Global Carbon Atlas, Fossil fuel emission database, **2017**.
http://www.globalcarbonatlas.org/en/CO2-emissions
(Accessed 02-01-2017)

22. Renewable Energy in the GULF: Facts and Figures, IRENA report, **2016**.
https://www.irena.org/DocumentDownloads/factsheet/Renewable%20Energy%20in%20the%20Gulf.pdf
(Accessed 02-01-2017)

23. K. C. Ng, W. Xiao-Lin, G. Lizhen, A. Chakraborty, B. B. Saha, A. Atsushi, K. Takao, US Patent # 2010/0258426A1.

24. K.C. Ng, K. Thu, A. Chakraborty, B.B. Saha, W.G. Chun, International Journal of Low-Carbon Technologies, **2009**, 4, 61-67.

25. K.C. Ng, K. Thu, B.B. Saha, A. Chakraborty, W.G. Chun, International Journal of Refrigeration, **2012**, 35, 685-693.

26. K.C. Ng, K. Thu, Y.-D. Kim, A. Chakraborty, G. Amy, Desalination, **2013**, 308, 161-179.

27. B. B. Saha, I. I. El-Sharkawy, M. W. Shahzad, K. Thu, L. Ang, K. C. Ng, Applied Thermal Engineering, **2016**, 97, 68-76.

28. L. Ang, K. Thu, A. B. Ismail, M. W. Shahzad, K. C. Ng, International Journal of Heat and Mass Transfer, **2016**, 92, 149-157.

29. M. W. Shahzad, K. C. Ng, K. Thu, B. B. Saha, W. G. Chun, Applied Thermal Engineering, **2014**, 72, 289-297.

30. M. W. Shahzad, K. Thu, Y. D. Kim. K. C. Ng, Applied Energy, **2015**, 148, 273-281.

31. M. W. Shahzad, K. Thu, K. C. Ng, C. W. Gee, Desalination and Water treatment, **2015**, 1-10.

32. K. C. Ng, K. Thu, S. J. Oh, L. Ang, M. W. Shahzad and A. B. Ismail, Desalination, **2015,** 356. 255–270.

33. M.W. Shahzad, A. Myat, C. W. Gee, K. C. Ng, Thermal Engineering, **2013**, 50, 670-676.

34. M. W. Shahzad, K. C. Ng and K. Thu, Environmental Science: Water Research & Technology, **2016**, 2, 206-212.

17

Appendix A

Equation	Remarks
Modeling equations for first evaporator	
$$[(M_{hw}.Cp_{hw})]\frac{dT_{hw}}{dt} = \left(\overset{\bullet}{m}_{hw}, h_{f,Thw,in}\right) - \left(\overset{\bullet}{m}_{hw}\, h_{f,Thw,out}\right) - h_{in,o}.A_{in,i}\left(T_{hw} - T_{tube,i}\right)$$	Energy balance for the hot water flowing inside the tubes of brine heater.
$$[(M_{HX,i}.Cp_{hx,i})]\frac{dT_{tube,i}}{dt} = h_{in,i}.A_{in,i}\left(T_{hw,i} - T_{tube,i}\right) - h_{out,i}.A_{out,i}\left(T_{tube,i} - T_{v,i}\right)$$	Energy balance for metal tubes.
$$\frac{dM_{b,i}}{dt} = \overset{\bullet}{m}_{f,i} - \overset{\bullet}{m}_{b,i} - \overset{\bullet}{m}_{v,i}$$	Mass balance for the seawater inventory in the evaporator side of the brine heater.
$$[(M_{b,i}.Cp_{b,Tb}) + (M_{HX,i}.Cp_{HX})]\frac{dT_i}{dt} = \left(\overset{\bullet}{m}_{f,i}\, h_{f,Tf}\right) - \left(\overset{\bullet}{m}_{b,i}\, h_{f,Tb}\right) - \left(\overset{\bullet}{m}_{v,i}\, h_{g,Tv}\right) + Q_{in,i}$$ $$Q_{in} = h_{o,i} A_i \left(T_t - T_{v,i}\right)$$	Energy balance for the evaporator side of the steam generator.
$$M_{b,i}\frac{dX_{b,i}}{dt} = \left(\overset{\bullet}{m}_{f,i}\, X_{f,i}\right) + \left(\overset{\bullet}{m}_{b,i}\, X_{b,i}\right) - \left(\overset{\bullet}{m}_{v,i}\, X_{v,i}\right)$$	Material/concentration balance
$$Nu = \frac{h_{in,i} d_{in,i}}{K_{tube,i}} = 0.023 \mathrm{Re}_l^{0.80}\, \mathrm{Pr}_l^{0.40}$$	Convective heat transfer coefficient equation
$$R_{wall,i} = \frac{\ln\left(\dfrac{d_{out,i}}{d_{in,i}}\right)}{2.\pi.K_{tube,i}.L_{tube,i}}$$	Tube wall resistance
$$U_i A_i = \frac{1}{\dfrac{1}{h_{in,i} A_{in,i}} + R_{wall,i} + \dfrac{1}{h_{out,i} A_{out,i}}}$$	Overall heat transfer coefficient
Modeling equations for intermediate evaporators	
$$[(M_{l,i+1}.Cp_{l,Tcond})]\frac{dT_{cond,i+1}}{dt} = \left[\overset{\bullet}{m}_{v,}\, h_{fg,Tv}\right]_i - \left[h_{in}.A_{in}\left(T_{cond} - T_{tube}\right)\right]_{i+1}$$	Energy balance for the condenser side of the ith effect.
$$[(M_{HX,i+1}.Cp_{hx,i+1})]\frac{dT_{tube,i+1}}{dt} = h_{in,i+1}.A_{in,i+1}\left(T_{cond,i+1} - T_{tube,i+1}\right) -$$ $$h_{out,i+1}.A_{out,i+1}\left(T_{tube,i+1} - T_{v,i+1}\right)$$	Energy balance for tube metal

18

$\dfrac{dM_{b,i+1}}{dt} = \overset{\bullet}{m}_{f,i+1} - \overset{\bullet}{m}_{b,i+1} - \overset{\bullet}{m}_{v,i+1}$	Brine inventory balance
$\left[\left(M_{b,i+1}.Cp_b\right) + \left(M_{HX,i+1}.Cp_{HX,i+1}\right)\right]\dfrac{dT_{i+1}}{dt} =$ $\left(\overset{\bullet}{m}_{f,i+!}\, h_{f,Tf}\right) - \left(\overset{\bullet}{m}_{b,i+1}\, h_{f,Tb}\right) - \left(\overset{\bullet}{m}_{v,i+1}\, h_{g,Tv}\right) + Q_{in,i+1}$ $Q_{in,i+1} = h_{out,i+1} A_{i+1}\left(T_{t,i+1} - T_{v,i+1}\right)$	Energy balance for evaporator side
$M_{b,i+1} \dfrac{dX_{b,i+1}}{dt} = \left(\overset{\bullet}{m}_{f,i+1}\, X_{f,i+!}\right) - \left(\overset{\bullet}{m}_{b,i+1}\, X_{b,i+1}\right) - \left(\overset{\bullet}{m}_{v,i+!}\, X_{v,i+!}\right)$	Material/ concentration balance
$Nu = \dfrac{h_{in,i+1}L_{i+1}}{K_{tube,i+1}} = 0.728\left[\dfrac{gh_{fg,Tcond}\,\rho_{l,Tcond}\left(\rho_l - \rho_v\right)_{Tcond} K_{l,Tcond}^3}{\mu_{l,Tcond}\,d_i\left(T_{v,i+1} - T_{tube,i+1}\right)}\right]^{1/4}$	Nusselt film condensation correlation for the calculation of the heat transfer coefficient inside the condenser tubes
$U_i A_i = \dfrac{1}{\dfrac{1}{h_{in,i}A_{in,i}} + R_{wall,i} + \dfrac{1}{h_{out,i}A_{out,i}}}$	Overall heat transfer coefficient equation.

Last evaporator integrated with AD cycle

$\left[\left(M_{b,n}.Cp_b\right) + \left(M_{HX,n}.Cp_{HX,n}\right)\right]\dfrac{dT_n}{dt} = \left(\overset{\bullet}{m}_{f,n}\, h_{f,Tf}\right) - \left(\overset{\bullet}{m}_{b,n}\, h_{f,Tb}\right) - \left(M_{sg}\, h_{g,Tv}\right)\dfrac{dq_{ads}}{dt} + Q_{in,n}$ $Q_{in,n} = h_{out,n} A_n\left(T_{t,n} - T_{v,n}\right)$	Energy balance for the condenser side of the ith effect.

19